Materials Characterization 106 (2015) 108–111

Contents lists available at ScienceDirect

Materials Characterization

journal homepage: www.elsevier.com/locate/matchar

Correlation between mechanical properties and retained austenite characteristics in a low-carbon medium manganese alloyed steel plate

Jun Chen [a,*], Mengyang Lv [b], Shuai Tang [a], Zhenyu Liu [a], Guodong Wang [a]

[a] State Key Laboratory of Rolling and Automation, Northeastern University, Shenyang 110819, People's Republic of China
[b] School of Materials and Metallurgy, Northeastern University, Shenyang 110819, People's Republic of China

ARTICLE INFO

Article history:
Received 13 January 2015
Received in revised form 11 May 2015
Accepted 19 May 2015
Available online 21 May 2015

Keywords:
Medium manganese steel
Transmission electron microscopy
Mechanical properties
Retained austenite

ABSTRACT

The effects of retained austenite characteristics on tensile properties and low-temperature impact toughness have been investigated by means of transmission electron microscopy and X-ray diffraction. It was found that only part of austenite phase formed during heat treating was left at room temperature. Moreover, the film-like retained austenite is displayed between bcc-martensite laths after heat treating at 600 °C, while the block-form retained austenite with thin hcp-martensite laths is observed after heat treating at 650 °C. It has been demonstrated that the film-like retained austenite possesses relatively high thermal and mechanical stability, and it can greatly improve low-temperature impact toughness, but its contribution to strain hardening capacity is limited. However, the block-form retained austenite can greatly enhance ultimate tensile strength and strain hardening capacity, but its contribution to low-temperature impact toughness is poor.

1. Introduction

Recently, the studies on retained austenite in conventional transformation-induced plasticity (TRIP), quenching and partitioning (Q&P) and medium manganese steels have dramatically increased. Moreover, these studies have mainly focused on the effects of chemical composition design and heat treatment on retained austenite characteristics and the correlation between retained austenite and tensile properties [1–18]. However, there have been few studies on the correlation between retained austenite characteristics and low-temperature impact toughness in low-carbon medium manganese steels.

For medium manganese steels, fully martensitic microstructure is commonly obtained even at a very low cooling rate [10]. Although this microstructure possesses high strength, it has poor ductility and toughness. It is well known that the outstanding combination of strength and ductility can be achieved by introducing retained austenite, and such ductility can be mainly achieved by TRIP effect of a large volume fraction of metastable retained austenite [8,12,19–24]. To produce retained austenite, the transformation from α' to γ which is termed austenite reverted transformation (ART) [1,24] is commonly used in medium manganese steels. Although the TRIP effect of metastable retained austenite has pronounced contributions to ductility and strain hardening capacity, whether it has the same contributions to low-temperature impact toughness has not been clarified. Zhou et al. [15] reported an increase in product strength and ductility accompanied by a large decrease in toughness, indicating that the influence of retained austenite on tensile properties is inconsistent with that on low-temperature impact toughness. On the one hand, the stacking fault energy of retained austenite decreases with lowering temperature [25], indicating that the stability of retained austenite is lowered. On the other hand, the deformation behavior of retained austenite during low-temperature impact test with a high strain rate may be different from that during room temperature tensile test with a relatively low strain rate. Hence, the present study intends to identify the effects of retained austenite characteristics on tensile properties and low-temperature impact toughness in low-carbon medium manganese steel.

2. Materials and methods

The chemical composition of the steel is Fe–0.035C–0.20Si–5.1Mn–1.4Ni (in mass %). The steel was melted in a vacuum induction furnace and cast into an ingot, which was hot forged into a square billet ($70 \times 70 \times 150$ mm^3). This square billet was homogenized in a box-type electrical resistance furnace at 1200 °C for 2 h, then hot rolled in six passes to a 12 mm thickness plate, and finally cooled to room temperature in water. After that, the hot rolled steel plate was isothermally treated at 600 °C or 650 °C for 2 h, where the Thermo-Calc calculation results show that two phases (ferrite and austenite) coexist, and then water quenched to room temperature.

Standard round tensile samples with the gauge length of 40 mm and diameter of 8 mm were prepared from heat treated steel plates along the rolling direction. Mechanical properties were measured using a CMT-5105 electron universal testing machine at room temperature at a cross beam speed of 3 mm/min. Standard Charpy V-notch (CVN) impact samples with the size of $10 \times 10 \times 55$ mm^3 were also prepared.

* Corresponding author.
E-mail address: cjer19841011@163.com (J. Chen).

http://dx.doi.org/10.1016/j.matchar.2015.05.026
1044-5803/

The CVN impact energy was measured using a JBW-500 impact tester at the temperatures of 15, −20, −40, −60, −80 and −100 °C. Moreover, the average yield strength, ultimate tensile strength, total elongation and CVN impact energy were determined using three tensile or CVN impact test data.

Transmission electron microscopy specimens were prepared by cutting slices with 500 μm thickness from the heat treated steel plates using electron discharge machine. These slices were mechanically thinned to 50 μm thickness from both sides using silica papers, followed by punching to prepare round disks with 3 mm diameter. Subsequently, the disks were further thinned using a twin-jet electropolisher (StruersTenuPol-5) at a voltage of 30 V and the temperature between −5 and 5 °C. The electrolyte consisted of 9% perchloric acid and 91% absolute ethyl alcohol. They were examined on a field-emission transmission electron microscope (FEI Tecnai G^2 F20) operated at 200 kV. In addition, the volume fractions of retained austenite were measured using X-ray diffraction (XRD) with a wavelength of 1.54056 Å. Samples for XRD analysis were mechanically polished at first and then electropolished in a mixture consisting of 12.5% perchloric acid and 87.5% absolute ethyl alcohol at room temperature to remove surface strain layer.

3. Results and discussion

The engineering stress–strain curves and corresponding strain hardening rates of the steel after heat treating at 600 °C or 650 °C for 2 h are shown in Fig. 1. It can be seen that the tensile properties strongly depend on heat treating temperature. The steel treated at 600 °C for 2 h shows the yield strength (lower yield stress) of 735 MPa, ultimate tensile strength of 787 MPa and total elongation of 24%. When the heat treating temperature increases to 650 °C, the yield strength (0.2% offset stress) decreases to 588 MPa, but the ultimate tensile strength increases to 915 MPa. Although the uniform elongation is marginally improved by increasing the heat treating temperature to 650 °C, the total elongation is nearly not improved. Note that the steel treated at 650 °C shows a lower yield ratio (0.64), indicating that it possesses an excellent strain hardening capacity. In contrast, the steel treated at 600 °C has a poor strain hardening capacity. In addition, the strain hardening rates were derived from true stress–strain curves, as shown in Fig. 1b, exhibiting that the strain hardening behavior also strongly depends on heat treating temperature. For the steel treated at 600 °C, the strain hardening rate sharply increases at first and then decreases at stage 1, and it nearly remains unchanged at stage 2. After that, the strain hardening rate sharply increases to ~2500 MPa at first and then linearly decreases at stage 3. For the steel treated at 650 °C, the steel shows a steep decrease in strain hardening rate below the true strain of 0.012. After that, the strain hardening rate linearly decreases from ~7500 MPa to ~2500 MPa in a higher slope at first and then continues to decrease in a lower slope with further increasing strain. Hence, the heat treating temperature which affects retained austenite characteristics plays a significant role in tensile properties.

The CVN impact energies of the steel after heat treating at 600 °C or 650 °C for 2 h are shown in Fig. 2, showing that the low-temperature impact toughness also strongly depends on the heat treating temperature. After heat treating at a relatively low temperature of 600 °C, the CVN impact energy almost remains unchanged above −40 °C, and below this point, it linearly decreases from ~250 J to ~160 J with further lowering temperature, indicating that the steel possesses outstanding low-temperature impact toughness. However, after heat treating at relatively high temperature of 650 °C, the CVN impact energy linearly decreases from ~164 J to ~80 J with lowering temperature. It is interesting to note that the steel with poor strain hardening capacity possesses excellent low-temperature impact toughness, while the low-temperature impact toughness of the steel with expected strain hardening capacity is not very good, indicating that the influence of retained austenite on tensile properties is inconsistent with that on low-temperature impact toughness. Zhou et al. [15] also reported that an increase in product of tensile strength and total elongation accompanied by a sharp decrease in toughness at room temperature in conventional TRIP steels. Seol et al. [14] reported the toughness of a high-carbon bainitic–austenitic TRIP steels and also indicated that a proper decrease in austempering temperature can improve toughness.

The bright- and dark-field TEM micrographs of the steel after heat treating at 600 °C for 2 h and the selected area diffraction pattern (SADP) are presented in Fig. 3. Extensive film-like retained austenite is displayed between bcc-martensite laths and only few block-form retained austenite grains are observed, suggesting that the retained austenite embryos mainly nucleated at lath boundaries during heat treating at a relatively low temperature of 600 °C. The austenite nucleation at lath boundaries is associated with co-segregation of carbon and manganese at lath boundaries [2] and the increment of elastic strain energy reduced with lowering reversion temperature [26]. Note that the average thickness of film-like retained austenite is 83 ± 30 nm, implying that it has sufficient stability [8]. In addition, Xiong et al. [12] also reported that the film-like retained austenite possesses an excellent stability. Fig. 3c and d shows that the orientation relationships between film-like retained austenite and α′ lath are $[001]_{\alpha'}//[011]_{\gamma}$ and $[110]_{\alpha'}//[-1\text{–}11]_{\gamma}$, i.e., one variant of Nishiyama–Wassermann (N–W) orientation relationship of $(-1\text{–}11)_{\gamma}//(110)_{\alpha'}$ and $[011]_{\gamma}//[001]_{\alpha'}$ [3,23,27].

The TEM micrographs of the steel after heat treating at 650 °C for 2 h and the SADP are presented in Fig. 4. It is worth noting that the retained austenite morphology is very different from that in Fig. 3. Extensive thin hcp-martensite (ε) laths are displayed inside block-form retained austenite, as shown in Fig. 4d, e and f. The existence of thin ε laths inside

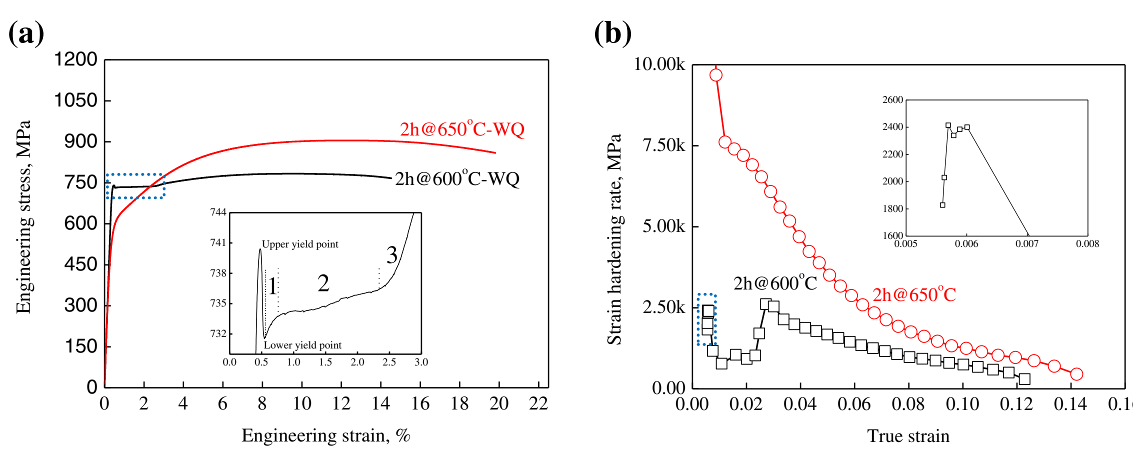

Fig. 1. (a) Engineering stress–strain curves and (b) strain hardening rates of the steel after heat treating at 600 °C or 650 °C for 2 h. The blank rectangles and circles represent the strain hardening rates derived from true stress–true strain curves of the steel treated at 600 °C and 650 °C for 2 h, respectively.